biomass

MDPI

Article

Biobased Composites from Starch and Mango Kernel Flour

Hálisson Lucas Ribeiro [1], Matheus de Oliveira Barros [2], Adriano Lincoln Albuquerque Mattos [2], Morsyleide de Freitas Rosa [2], Men de Sá Moreira de Souza Filho [2] and Henriette Monteiro Cordeiro de Azeredo [3,*]

1 Department of Chemical Engineering, Pici Campus, Building 709, Av. Mister Hull, Pici, Fortaleza 60455-760, CE, Brazil; halissonlucas@gmail.com
2 Embrapa Tropical Agroindustry, R. Dra. Sara Mesquita, 2270, Pici, Fortaleza 60511-110, CE, Brazil; matheus_barros@outlook.com (M.d.O.B.); adriano.mattos@embrapa.br (A.L.A.M.); morsyleide.rosa@embrapa.br (M.d.F.R.); men.souza@embrapa.br (M.d.S.M.d.S.F.)
3 Embrapa Instrumentation, R. 15 de Novembro, 1452, Centro, São Carlos 13561-206, SP, Brazil
* Correspondence: henriette.azeredo@embrapa.br; Tel.: +55-(16)-2107-2800

Abstract

Starch is a promising alternative to petroleum-based polymers due to its biodegradability and renewable nature. However, its widespread use in non-food applications raises ethical concerns. Mango kernels, a major byproduct of mango processing, represent an abundant yet underutilized starch source. However, conventional starch extraction requires costly purification steps with significant environmental impact. This study explores the development of extruded biocomposites, using corn starch and mango kernel flour (MKF) as a more sustainable alternative. The influence of lignin, extractives, amylose, and amylopectin content on the material properties was assessed. MKF was obtained by removing both tegument and endocarp from the mango kernels, grinding them in a colloidal mill, and finally drying the ground kernels. The resulting flour was blended with corn starch, processed in an internal mixer, and injection-molded. The composites were characterized through mechanical testing, water absorption analysis, colorimetry, and UV absorption assays. Notably, the composite containing ~20% MKF exhibited mechanical properties comparable to commercial polyethylene (PE-PB 208), with a tensile strength of 9.53 MPa and a Young's modulus of 241.41 MPa. Additionally, MKF enhanced UVA protection. These findings suggest that mango kernel flour can partially replace starch in the production of injection-molded biopolymers, offering a more sustainable approach to biodegradable plastic development.

Keywords: biodegradable polymers; food waste; mango kernel flour; starch-based bioplastics; thermoplastics development

Academic Editor: Fabrizio Scala

Received: 20 August 2025
Revised: 23 September 2025
Accepted: 2 October 2025
Published: 10 October 2025

Citation: Ribeiro, H.L.; Barros, M.d.O.; Mattos, A.L.A.; Rosa, M.d.F.; Filho, M.d.S.M.d.S.; Azeredo, H.M.C.d. Biobased Composites from Starch and Mango Kernel Flour. *Biomass* **2025**, *5*, 64. https://doi.org/10.3390/biomass5040064

1. Introduction

Plastic waste generation exceeds 460 million tons annually, posing serious threats to ecosystems, the climate, and human health. Despite efforts to improve recycling, most of the plastic waste is either landfilled (46%) or improperly managed, with only 10% undergoing recycling. In response, global policies, including the UN's 2024 General Assembly resolution that calls for circular economy practices and regulations in the EU, China, the US, and Brazil, aim to mitigate plastic pollution by encouraging the development of sustainable alternatives [1–3].

Starch, a plant-generated polysaccharide used to store energy, is found in large quantities in agricultural crops such as maize, wheat, rice, potato, sweet potato, cassava, and as

by-products in some fruit seeds [4–9]. Due to its widespread availability and high agricultural production, starch is a compelling substitute for petroleum-based polymers across various industries, including agriculture and healthcare. Starch is an essential component of both human and livestock diets. However, its diversion for non-food applications raises ethical concerns, as it could affect the global food supply and contribute to food security challenges [10]. Nevertheless, starch is abundantly found in non-edible products, numerous wild plant species, and crops cultivated specifically for non-edible purposes [2,10].

Mango (*Mangifera indica*) is one of the most important fruits in global agribusiness, with production reaching nearly 50 million metric tons in 2021, of which India accounts for 42% [11]. Mango kernel, the main byproduct of mango processing, has an estimated global annual yield of 123,000 metric tons [12]. Since the 1980s, it has been investigated as an alternative starch source, and in the past decade, the first studies exploring its use in thermoplastic production have been published [13,14].

Starch-based bioplastics presents a viable alternative to petroleum-derived polymers due to their biodegradability, renewability, and widespread availability. However, since starch is a staple food source for both humans and livestock, its use in non-food industrial applications raises ethical concerns. While mango kernel starch (MKS) has been explored as a sustainable alternative, its low extraction yield (32%) and the high environmental impact of its purification process hinder large-scale application. A viable alternative approach is the use of mango kernel flour (MKF), which retains native starch along with other components, potentially reducing the need for extensive purification while maintaining desirable material properties [11].

To enhance the efficiency of MKS utilization, some studies have developed MKF films using the casting process. Gomez-Caturla et al. [15] studied the effect of flour particle size on MKF film properties, highlighting significant antioxidant activity with potential applications in food packaging. Additionally, existing research emphasizes the antimicrobial properties of mango kernel extractives, along with their potential health benefits, including anticancer, antidiabetic, and anti-inflammatory properties. These findings broaden the scope for mango kernel-derived compounds in the development of innovative and multifunctional products [16].

This study aims to develop extruded biopolymer composites by combining MKF with corn starch (CS). Corn starch was chosen as the matrix component due to its availability, cost-effectiveness, and widespread use in thermoplastic applications, making it a suitable base to blend with MKF [11,12]. Additionally, its higher amylose content plays a crucial role in optimizing properties, as the mechanical and thermal behavior of starch-based composites depends on the amylose–to–amylopectin ratio. Meanwhile, MKF contributes with extractives and lignin, which may enhance composite performance. This strategic combination harnesses the advantages of both materials developing a more sustainable and functional biopolymer [11].

By incorporating MKF into starch-based composites, this study explores a more sustainable and cost-effective alternative to purified MKS-based bioplastics. The resulting materials were characterized regarding their mechanical properties, water absorption, color stability, and UV resistance, to assess their suitability for potential applications in biopolymer development.

2. Materials and Methods

2.1. Schematic View

Figure 1 shows the schematic representation of this work, highlighting its process and concept.

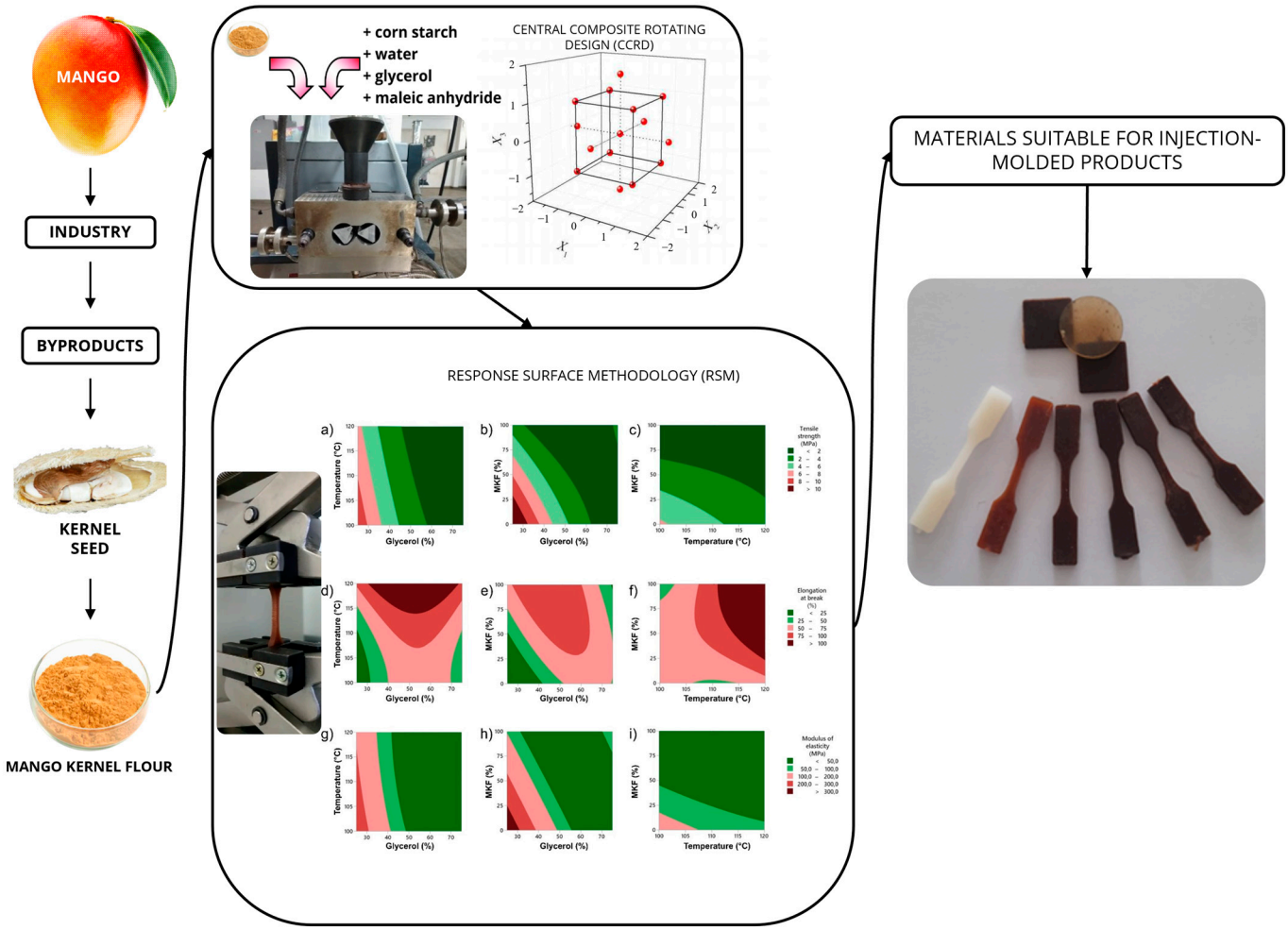

Figure 1. Schematic representation of the research workflow. Mango byproducts were used for kernel flour production, processed and combined with starch. The mixtures were molded, mechanically tested, and analyzed through statistical models, resulting in materials suitable for injection-molded applications.

2.2. Materials

The mangoes (cv Tommy Atkins) used in this work were purchased from the Central Supplying Station of Ceará (CEASA, in Maracanaú, CE, Brazil). Additionally, commercially available corn starch (Kimimo, Eusébio, CE, Brazil), glycerol, maleic anhydride, and Dicumyl peroxide (SIGMA Aldrich, Saint Louis, MO, USA) were used.

2.3. Production of Mango Kernel Flour (MKF)

To produce MKF, the mangoes were processed by first separating the pulp from the skin and stones. The tegument and the endocarp were then removed from the kernels, which were then treated with a 0.05% (*w*/*v*) sodium metabisulfite solution for 24 h, followed by drainage. The treated kernels were then ground with water (1:1 weight ratio) using an Ultra Turrax T50 (Ika, Staufen, Germany) at 5000 rpm for 5 min. The resulting slurry was processed in a Colloidal Mill (Nova Meteor-REX 1-N, Meteor Indústria e Comércio Ltda, São Paulo, Brazil) to form a paste, which was subsequently dried in a forced-air oven at 40 °C for 48 h. The dried paste was then powdered using a knife mill (Pulverisette 16, Fritsch, Pittsboro, NC, USA).

2.4. Extraction of Mango Kernel Starch (MKS)

For MKS, the pulp was separated following the same procedure as described above. Kernels were extracted from the stones and immersed in 0.05% (*w*/*v*) sodium metabisulfite solution for 24 h, then drained. The kernels were ground with water at a 1:1 ratio using an Ultra Turrax T50 (Ika, Staufen, Germany) for 10 min at 8000 rpm, sieved, and repeatedly washed until the wash water was clear. The amylaceous fraction, allowed to sediment for 1 h, was treated with 0.2% (*w*/*v*) NaOH at a 1:2 weight ratio and stirred at 200 rpm for 2 h. The pH was then adjusted to 7.0 using 0.5% (*v*/*v*) HCl. After further sedimentation and washing, ethanol was added at a 1:2 weight ratio, and the mixture was stirred for 1 h. The starch was collected by vacuum filtration through 28 µm filter paper, dried at 40 °C for 24 h, and milled using a knife mill.

2.5. Chemical Characterization

The ash, extractives, proteins and lignin contents of MKF, MKS and CS were determined.

2.6. Amylose Content

The amylose content was assessed using methods described by Barros et al. [17]. First, 0.1 g of starch, 1 mL of absolute ethanol, and 10 mL of a solution of sodium hydroxide 1 M were combined, heated at 70 °C for 15 min, shaken at 5 min intervals, and cooled to room temperature. For the reaction, 0.5 mL of solubilized starch, 2 mL of iodine solution (I2 + KI; 0.01 M), 1 mL of acetic acid solution 1 M, and 46 mL of water were mixed and left at room temperature for 10 min. Absorbance was read at 620 nm in a spectrophotometer (Shimadzu UV 2450, Saint Louis, MO, USA) using 1.4 mL of the reaction mix and 1.4 mL of water, against a calibration curve. Water-only blank was used.

2.7. Thermogravimetric Analysis (TGA)

Thermal properties of raw material samples (~10 mg) were measured in a thermogravimetric analyzer STA 6000 (PerkinElmer, Waltham, MA, USA), under nitrogen atmosphere (40 mL/min), and heating rate of 10 °C.min^{-1}, from 25 °C to 800 °C.

2.8. Fourier Transform Infrared Spectroscopy Analysis (FTIR)

The infrared spectra of CS, MKF, and MKS were recorded in a FTIR spectrophotometer Spectrum Two (PerkinElmer). The samples were pelletized with KBr. The runs were performed on wavelengths of 4000 to 400 cm^{-1}, 32 runs, and resolution of 4 cm^{-1}.

2.9. Obtaining the Composites

Composite formulations followed a Central Composite Rotating Design (CCRD) with three independent variables: glycerol concentration in the glycerol/water mixture, varying from 25 to 75%, processing temperature between 100 and 120 °C; and MKF in the MKF/starch mixture, varying from 0 to 100%. Corn starch was used in this process due to difficulties in obtaining sufficient MKS at a lab scale. The biopolymer/plasticizer ratio was fixed at 70:30.

Table 1 shows the levels coded for process conditions according to Minitab® 15 software (Minitab Inc., State College, PA, USA). Samples were mixed in a Haake Rheomix 600 OS (Thermo Scientific, Waltham, MA, USA) equipped with a roller rotor at 60 rpm for 5 min. Maleic anhydride (1%) and dicumyl peroxide (0.5%), based on the total weight of CS, MKF, and glycerol, served as compatibilizer and radical initiator, respectively. Dry and liquid ingredients were pre-mixed, then combined and processed. The resulting material was cooled and prepared for injection-molding.

Table 1. Experimental design and treatment descriptions: glycerol concentration in the plasticizer mixture (%), processing temperature (°C), and MKF concentration in the matrix mixture (%).

Treatment	Glycerol (%)	Temperature (°C)	MKF (%)	Glycerol (%)	Temperature (°C)	MKF (%)
	Coded			Uncoded		
1	−1	−1	−1	35.12	104.05	20.24
2	1	−1	−1	64.88	104.05	20.24
3	−1	1	−1	35.12	115.95	20.24
4	1	1	−1	64.88	115.95	20.24
5	−1	−1	1	35.12	104.05	79.76
6	1	−1	1	64.88	104.05	79.76
7	−1	1	1	35.12	115.95	79.76
8	1	1	1	64.88	115.95	79.76
9	−1.68	0	0	25	110	50
10	1.68	0	0	75	110	50
11	0	−1.68	0	50	100	50
12	0	1.68	0	50	120	50
13	0	0	−1.68	50	110	0
14	0	0	1.68	50	110	100
15	0	0	0	50	110	50
16	0	0	0	50	110	50
17	0	0	0	50	110	50

2.10. Injection-Molding

The thermoplastic starch composite samples were injection-molded in a MiniJet II (Haake Thermo Scientific) in type V form according to ASTM D638. Process temperatures, pressures, and times were tuned for well-formed specimens across all formulations.

2.11. Tensile Tests

ASTM V specimens were stored at 50 ± 5% RH and 23 ± 2 °C for 7 days before mechanical tests in a universal testing machine (Emic DL-3000, EMIC, São José dos Pinhais, Brazil), with a 5 kN load cell and a crosshead speed of 10.0 mm/min, according to ASTM D638-14 [18]. The samples were stored for 48 h in a chamber with controlled RH (50 ± 5%) and temperature (23 ± 2 °C) prior to the analysis, to ensure that all the samples had the same moisture content during the analysis

2.12. Water Absorption Tests

Water absorption tests followed ASTM D570 [19], using triplicate injected probe disks (D = 25, h = 1.5 mm). They were oven-dried at 50 °C for 24 h, weighted (dry weight), soaked in water for 2 h, paper towel-dried, weighted (wet weight), and re-weighted after another 24 h of oven-drying (re-dried weight). The percentage of water absorption (*WA*) was the sum of the increase in weight on immersion (*IW*) and the soluble matter lost (*SML*):

$$WA(\%) = IW + SML \quad (1)$$

The *IW* was calculated according to the following equation:

$$IW(\%) = \frac{wet\ weight - dry\ weight}{dry\ weight} \times 100 \quad (2)$$

The *SML* was calculated according to the following equation:

$$SML(\%) = \frac{dry\ weight\ -\ re-dried\ weight}{dry\ weight} \times 100 \quad (3)$$

2.13. Color Parameter and Visual Appearance

The analysis of the L*, a*, and b* parameters (color system CIEL*a*b*) of the injection-molded specimens was performed using a Konica Minolta CM-5 colorimeter (JP TOWER, Chiyoda-ku, Tokyo, Japan).

2.14. Ultraviolet (UV) Absorption Tests

Disk-shaped composites (D = 25, h = 1.5 mm) were pressed at 17.5 kgf/cm^2 using a hydraulic press (Marconi, MA 098/50A/1). UV-Vis spectra were recorded in transmission mode by using a Shimadzu UV-2450 spectrophotometer equipped with an ISR-2200 integrating sphere attachment. UV protection percentages (SUV) in three wavelength regions (S_{UVA}: 320–400 nm, S_{UVB}: 280–320 nm, S_{UVC}: 200–280 nm) were calculated using the following equations [20]:

$$S_{UVA} = 1 - T_{UVA} = 1 - \frac{\sum_{320}^{400} T_\lambda \times \Delta\lambda}{\sum_{320}^{400} \Delta\lambda} \times 100\% \quad (4)$$

$$S_{UVB} = 1 - T_{UVB} = 1 - \frac{\sum_{280}^{320} T_\lambda \times \Delta\lambda}{\sum_{280}^{320} \Delta\lambda} \times 100\% \quad (5)$$

$$S_{UVC} = 1 - T_{UVC} = 1 - \frac{\sum_{200}^{280} T_\lambda \times \Delta\lambda}{\sum_{200}^{280} \Delta\lambda} \times 100\% \quad (6)$$

T_{UVA}, T_{UVB}, and T_{UVC} correspond to the mean transmittance percentage in the three regions, λ and $\Delta\lambda$ are the wavelength and wavelength dispersion, respectively, and T_λ is the spectral transmittance.

2.15. Statistical Analysis

Response Surface Methodology (RSM) was employed to analyze the impact of glycerol and water content, processing temperature, and MKF-CS ratio on the mechanical properties of thermoplastic starch composites. Treatments were performed in random order, and the data were analyzed using a response surface regression procedure.

For each response, contour plots were produced from regression equations for each two variables, keeping the third one at its central level (coded as 0). Minitab 15® software (Minitab Inc., State College, PA, USA) was used to conduct statistical analyses, and surface plotting. The models were checked for adequacy based on ANOVA and the F-test at 95% confidence level, and for their determination coefficients (R^2 values).

3. Results and Discussion

Chemical analysis of MKF (Table 2) revealed starch, protein, and extractive contents of 46.12%, 6.05%, and 22.24%, respectively. In other published works, starch contents have been reported to vary from 53.34 to 76.81%, and protein contents from 6.74 to 10.48% [11,21]. The extractive portion has been reported to include 7.81 to 13.6% lipids [11,21].

Table 2. Chemical composition of corn starch, mango kernel flour and mango kernel starch.

	CS	MKF	MKS
Moisture (%)	4.13 ± 0.15 ^{a}	5.95 ± 0.08 ^{b}	12.27 ± 0.27 ^{c}
Ash (%)	0.08 ± 0.01 ^{a}	1.39 ± 0.27 ^{b}	0.11 ± 0.02 ^{b}
Extractives (%)	0.65 ± 0.17 ^{a}	22.24 ± 0.50 ^{b}	6.29 ± 0.89 ^{c}
Insoluble lignin (%)	0.94 ± 0.21 ^{a}	12.05 ± 5.69 ^{a}	9.12 ± 0.02 ^{a}
Protein (%)	0.44 ± 0.05 ^{a}	6.05 ± 0.57 ^{b}	0.36 ± 0.01 ^{a}
Starch	81.53 ± 0.48	46.12 ± 7.48	71.61 ± 1.23
Amylose (%)	23.51 ± 0.49 ^{a}	3.82 ± 0.14 ^{b}	12.45 ± 0.42 ^{c}

Results are denoted as mean ± SD; different letters along the line indicate significant differences ($p < 0.05$).

MKS analysis revealed lower lignin and extractives than in MKF, as expected from the purification process. Amylose was higher in CS, impacting material properties like stress strength and Young's modulus, but reducing deformation at rupture [22]. Lignin, ash, and protein levels in MKF come from the kernel compositions.

Thermogravimetry (Figure 2) displayed an event before 130 °C related to water evaporation, for all samples. MKF had two subsequent events: one at 225 °C, likely due to extractive and protein degradation, and another at 275 °C and peaking at 320 °C, tied to starch degradation, which is known to occur around 300 °C. MKS presented a related peak with the same T_{onset} and a peak at 327 °C. The literature presents different results, i.e., T_{onset} for MKS at 296, 300, and 313.5 °C [23]. The variation may be related to different varieties of mango used to extract the starch. The starch degradation at this range of temperature is the cleavage of α-D-(1→4) and α-D-(1→6) glycosidic linkages and the disruption of hydrogen bonds [22]. CS presented the degradation T_{onset} at 280 °C and peak at 323 °C. The last event for MKF presented a T_{onset} at 365 °C and a peak at 400 °C, probably related to the degradation of cellulose, hemicellulose, and the partial loss of lignin from the sample [24].

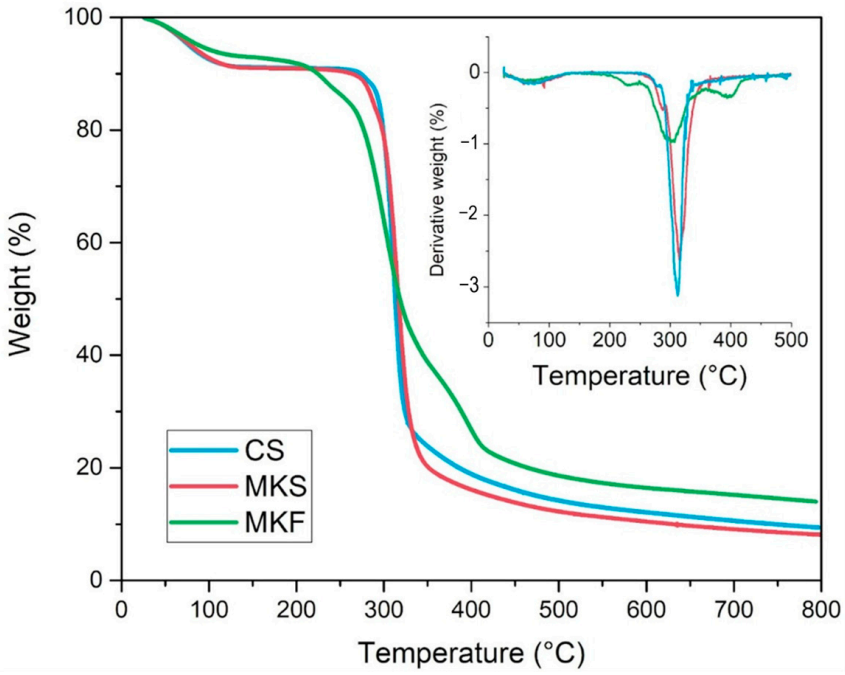

Figure 2. Thermogravimetric profiles of corn starch (CS), mango kernel starch (MKS), and mango kernel flour (MKF).

The FTIR spectra of the CS, MKS, and MKF are in Figure 3. The bands at 3400 and 2930 cm^{-1} are characteristic of the hydroxyl groups and of the CH bonds in glucose, respectively. The absorbance at 1645 cm^{-1} is due to the residual bounded water [25]. The absorption bands at 1155, 1080, 1020, and 930 cm^{-1} were attributed to the CO stretching vibration of starch [26]. The presence of α-1, 6-D-glucosidic and α-1, 4-D-glucosidic linkages is indicated by absorption at 925 cm^{-1} and 760 cm^{-1}, respectively [25]. At 1525 cm^{-1}, the MKF presents a different band that is related to aromatic compounds, present in the lignin of plant cell walls. Overall, no unusual bands were detected, indicating the purity of the samples used in this study [27].

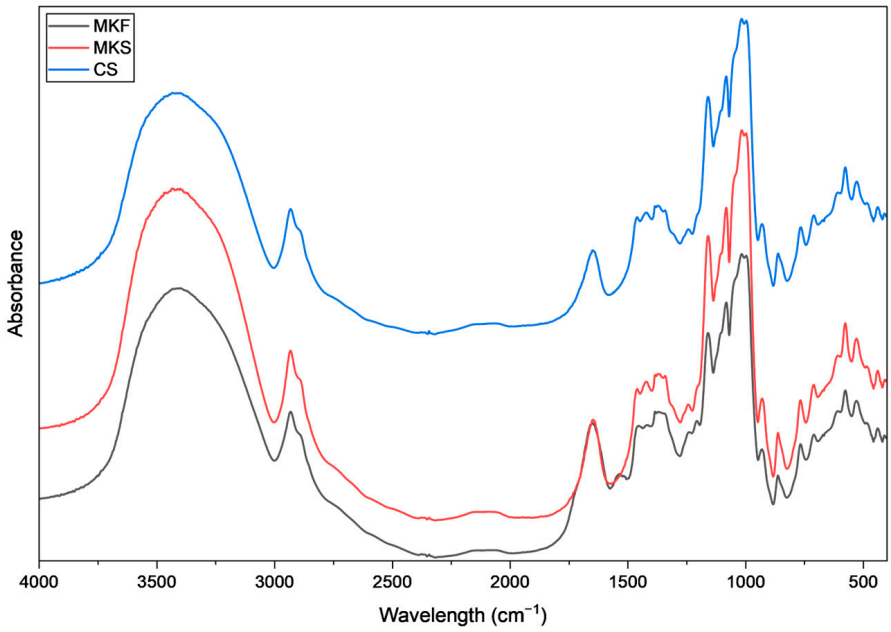

Figure 3. FTIR profiles of corn starch (CS), mango kernel starch (MKS), and mango kernel flour (MKF).

The composites were mixed in a Haake Rheomix chamber and molded into V-shaped specimens. Tensile strength ranged from 0.67 to 9.53 MPa. Figure 4 shows the tensile test curves for Treatments 13, 11, and 14, which contain 0%, 50%, and 100% MKF, respectively (Table 1). These three curves are presented as representative of the study.

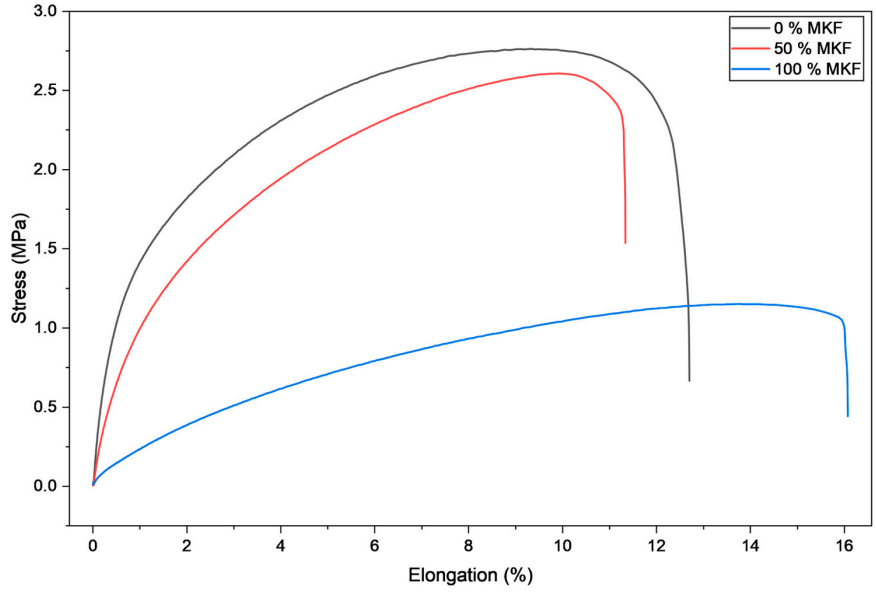

Figure 4. Tensile test curves for samples containing 0%, 50%, and 100% MKF in their composition.

Response surface analysis (Figure 5) showed that low glycerol and MKF concentrations increased tensile strength and Young's modulus. Otherwise, higher glycerol and MKF concentrations resulted in lower tensile strength and Young's modulus, and higher elongation at break. A similar behavior (glycerol into a starch matrix decreasing the intramolecular interactions and increasing the starch polymer chain mobility) was described before [28,29]. Glycerol is known as a plasticizer not just by turning the starch granules into thermoplastic starch, as it remains in the TPS matrix, but also by promoting a decrease in tensile strength and Young's modulus, and an increase in elongation at break (Figure 5). The decrease in tension strength and Young's modulus followed a parabolic trend, while the increase

in elongation at break exhibited negative quadratic behavior with a distinct maximum. Amylose concentration also influenced mechanical properties [30], with lower amylose concentration in MKF resulting in lower tensile strength and Young's modulus, and higher elongation at break, which is due to lower branching of amylose when compared to that of amylopectin, resulting in a more compact structure.

By examining the designed treatments, it was found that the addition of 20.24% MKF resulted in comparable tensile strength (9.53 MPa) and Young's modulus (241.41 MPa) to polyethylene PB 208, a commercially available polymer with a tensile strength of 10 MPa and Young's modulus of 250 MPa. This polymer is well-suited for injection-molded flexible parts.

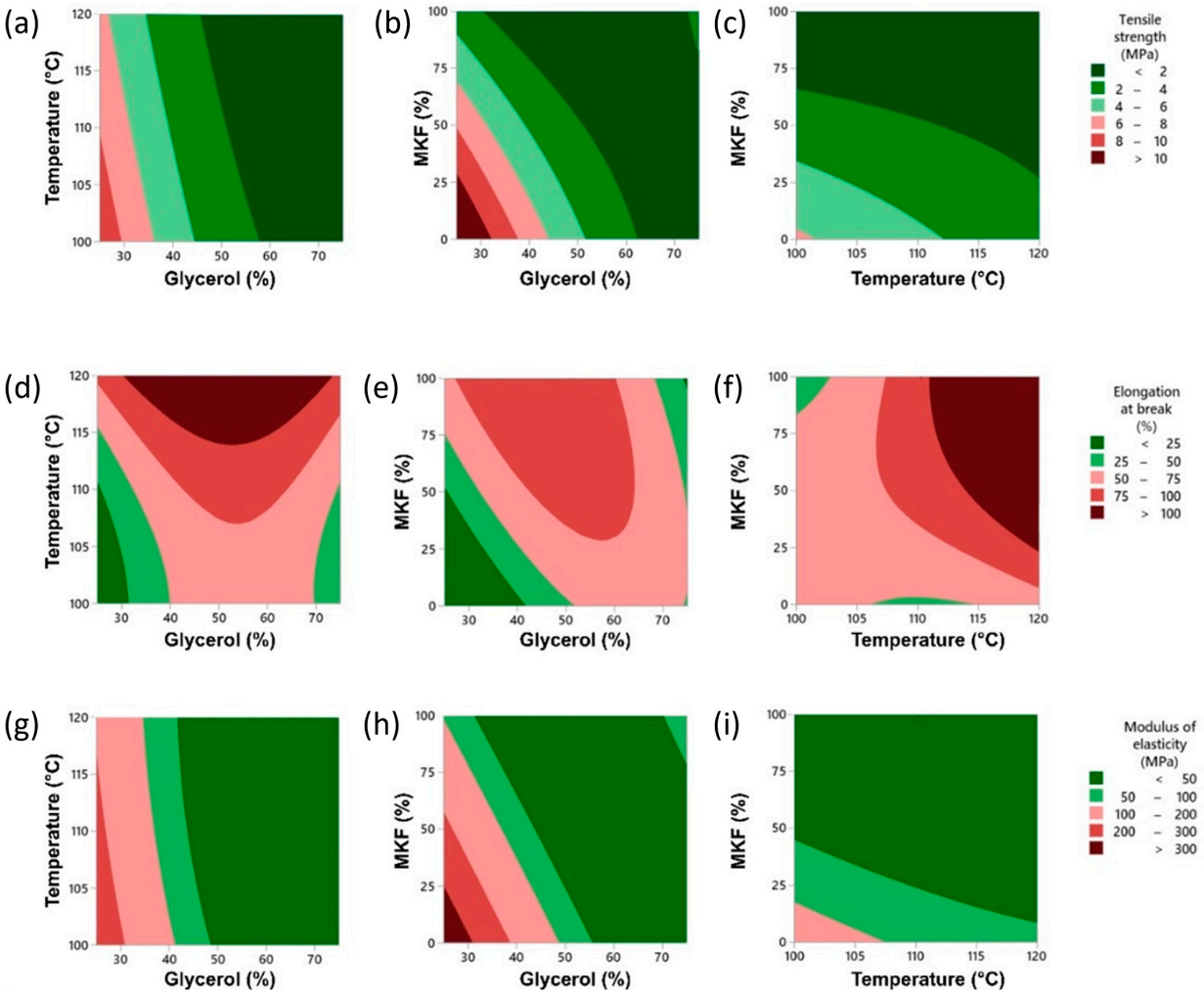

Figure 5. Graphical representation of the regression models for the tensile strength (**a**–**c**), enlogation at break (**d**–**f**), and modulus of elasticity (**g**–**i**) of the composites obtained in the mixing chamber.

Low temperatures do not sufficiently plasticize starch during extrusion, while high temperatures rapidly evaporate moisture, inhibiting full plasticization [31]. All treatments maintained a constant plasticizer–to–matrix ratio, differing only in glycerol concentration. Higher glycerol meant less water in the plasticizer mix, leading to higher tensile strength and Young's modulus but lower elongation at break, aligning with anti-plasticization phenomena. Water molecules are adsorbed around glycerol hydroxyl groups, generating a plasticizer effect [32]. But when water concentration is excessive, the branches of the starch macromolecule move closer together, reducing chain mobility [33].

Non-plasticized starch granules act as fillers in the TPS matrix, so the elongation behavior of TPS materials reflects its plasticization degree. By observing Figure 5d, it is possible to identify an optimal glycerol concentration, where greater elongations are possible at lower temperatures. This is evidence that this water/glycerol ratio optimizes the starch plasticization process. The soluble matter loss in water is another aspect related to the plasticization process [6]. Soluble matter loss was higher at lower temperatures (Figure 6), increasing the concentration of glycerol. Alonso-González et al. [6], processing rice bran at 80 °C, found the same behavior. Concerning the use of MKF in the treatments, as the concentration of MKF increases, less matter loss occurs with lower glycerol concentrations.

The fresh mango kernel is light yellow colored, but after processing, Maillard reactions affect low-mass sugars and proteins [5]. The MKF itself has a light brown color. The color changes become stronger after processing. Measurements of the a* coordinate describe changes from red if positive to green if negative. The b* positive values indicate a yellow component in the color, while negative values mean a blue component. Analysis of the significant values of the regressions (Table 3) revealed a positive linear effect and a negative quadratic effect of the presence of MKF on the a* and b* color parameters, suggesting that the addition of MKF is contributing to the direct change in color characteristics. After a certain point, there is a reduction in the effect, indicating a more complex relationship between the parameters.

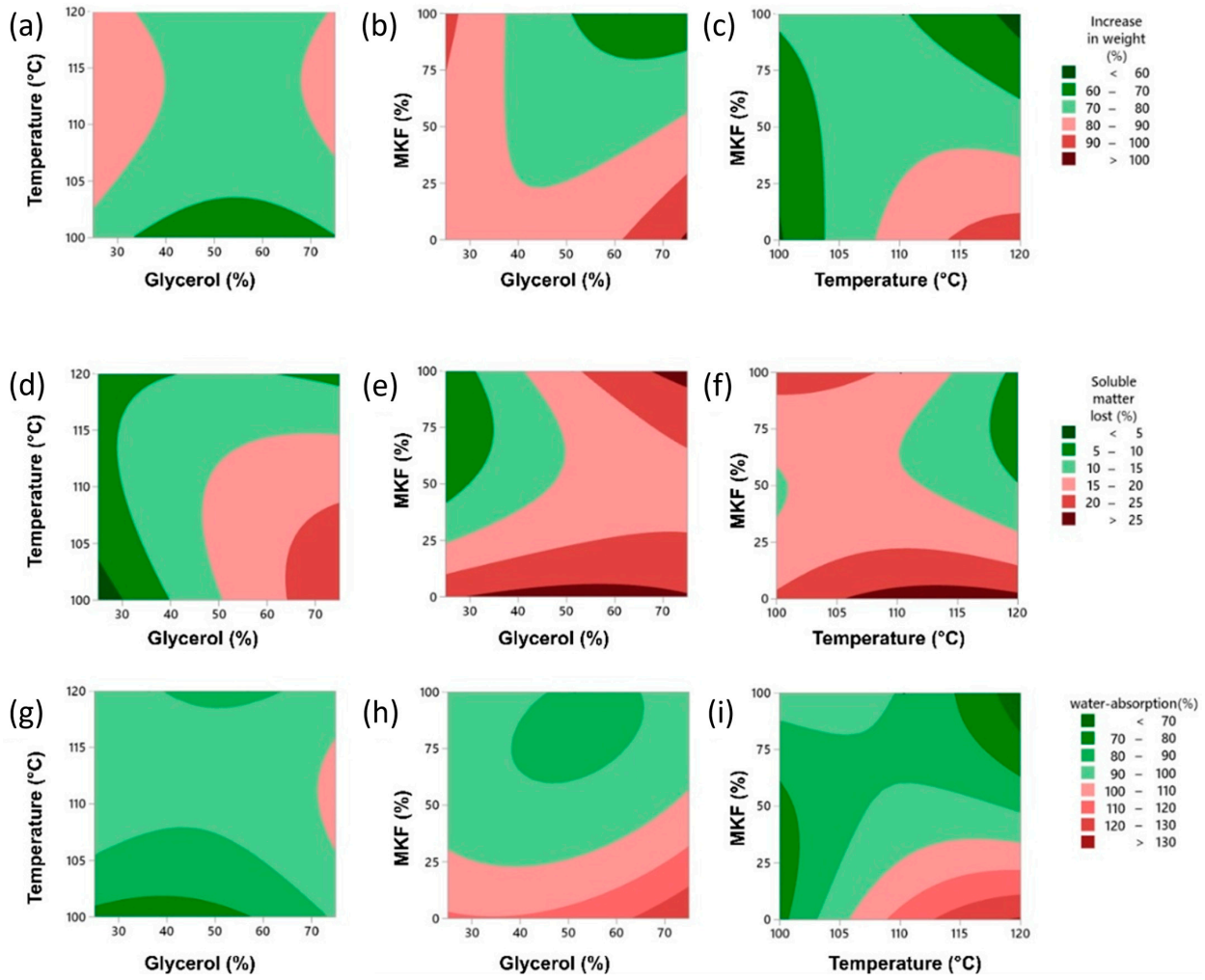

Figure 6. Graphical representations of the regression models for Increase in weight (**a**–**c**), Soluble matter lost (**d**–**f**), and Water absorption (**g**–**i**) of the composites obtained in the mixing chamber.

UV light protection in food packaging serves multiple purposes. It shields packaged food from UV radiation, which can degrade products, generate free radicals, and cause lipid oxidation, leading to unpleasant taste, discoloration, and nutritional loss [34]. Therefore, incorporating UV protection in packaging is essential for maintaining food quality and safety.

Analysis of the regressions (Table 3) indicates the significance of the model, suggesting its usefulness in predicting the UVA barrier. The MKF shows a significant linear contribution, evidencing its considerable effect on the UVA barrier. The quadratic contribution of MKF suggests a parabolic relationship and the possible presence of an optimal value where the barrier to UVA is maximized. Analysis of the raw data indicates that the composites possess barrier properties against UVA, UVB, and UVC.

MKF appears relevant mainly in the UVA barrier, but not as much in the UVB or UVC barriers. Glycerol, temperature, and MKF may still have an impact even if they were not significant in the regression models. The relationships between these variables and the UV barriers may be complex and not suitable for the regression model used, and it is even possible that unconsidered variables, such as the crystallinity of the composites or the presence of other elements, also exerted an influence. Lignin, a natural complex polymer present in various lignocellulosic feedstock materials, has been associated with the absorption of UV radiation [35]. Consequently, the lignin content in the MKF could contribute to the observed UV barrier properties.

Table 3. Coefficients for the regression model for process parameter and product response.

Terms	Tensile Strength (MPa)	Elongation at Break (%)	Modulus of Elasticity (MPa)	Increase in Weight (%)	Soluble Matter Lost (%)	Water Absorption (%)	L*	a*	b*	UVA Shielding (%)	UVB Shielding (%)	UVC Shielding (%)
Constant	**2.13**	**83.07**	17.90	**76.57**	**15.58**	**92.10**	**34.89**	**8.78**	**10.85**	**97.4**	**99.39**	**99.74**
X1	**−3.21**	12.80	**−102.20**	−2.66	**5.39**	3.02	−1.44	0.28	−0.33	−7.53	2.04	2.99
X2	−0.76	**35.43**	−14.50	5.26	**−2.20**	5.49	−0.66	**1.10**	0.21	−4.29	−2.68	−4,5
X3	**−2.10**	**23.15**	**−50.80**	−6.70	**−3.99**	−12.01	1.28	**3.75**	**4.30**	**28.84**	6.11	−3.81
$X1^2$	**2.54**	**−47.90**	**101.90**	8.20	−1.95	7.20	0.56	0.04	0.92	−16.68	−6.1	−17
$X2^2$	0.11	17.50	9.90	−7.00	−3.13	−9.40	2.57	0.43	1.90	−0.56	5.4	1.3
$X3^2$	0.16	−13.30	21.20	0.70	**7.25**	9.20	0.96	**−4.38**	**−5.27**	**−35.54**	−15.4	0.4
X1*X2	0.77	−5.50	25.30	0.30	**−5.17**	−4.00	−1.90	−0.05	−0.40	−5.8	−7.7	−12.8
X1*X3	**2.89**	**−37.10**	**96.40**	−11.80	**4.85**	−6.10	0.22	0.38	1.06	1.7	−7.6	−12.7
X2*X3	1.06	**37.00**	24.00	−12.80	**−4.81**	−21.80	−1.69	−0.28	1.19	−6.5	−7.6	−12.8
Freg	9.09	8.79	19.61	0.45	13.90	0.58	1.59	17,81	8.73	7.21	0.52	0.84
p	**<0.01**	**<0.01**	**<0.01**	0.87	**<0.01**	0.78	0.28	**<0.01**	**<0.01**	**<0.01**	0.82	0.606
R2 (%)	92.12	91.87	96.18	36.43	94.70	42.73	67.11	95.81	91.82	90.26	40.21	51.89

X1: Glycerol (%); X2: Temperature (°C); X3: MKF (%); Freg: F value for regression and the respective *p* value; R2: coefficients of determination. Bold values are significant at $p < 0.05$. Statistical analysis was able to describe the influence of the chosen parameters (Glycerol, temperature, and MKF) on tensile strength; elongation at break; Young's modulus; soluble matter loss; CIELAB components a* and b*; and UVA, UVB, and UVC shielding, as the significances observed were less than 5% (*p*-value < 0.05).

4. Conclusions

The mango kernel flour/corn starch composite from Treatment 1 (35.12% glycerol in the plasticizing mixture and processing temperature of 104 °C, and 20.24% MKF) exhibited mechanical properties comparable to polyethylene PB 208, achieving a tensile strength of 9.53 MPa and a Young's modulus of 241.41 MPa. In addition, MKF improved UVA protection. However, due to its starch-based nature, the material is best suited for use in low-humidity environments, making it ideal for packaging dry products such as flour, biscuits, and cereals. MKF can also partially substitute starch in injection-molded biopolymers, offering a more sustainable approach to the development of biodegradable plastics. These results underscore the potential for further optimization of processing parameters and formulation to deliver environmentally friendly, socially responsible, and economically viable packaging solutions.

Author Contributions: H.L.R. (conceptualization, data curation, formal analysis, investigation, writing—original draft), M.d.O.B. (visualization; writing—review and editing), A.L.A.M. (conceptualization, formal analysis, investigation, project administration, supervision, writing—review and editing), M.d.F.R. (conceptualization, formal analysis, funding acquisition, investigation, project administration, supervision, writing—review and editing), M.d.S.M.d.S.F. (conceptualization, formal analysis, funding acquisition, investigation, project administration, supervision, writing—review and editing) and H.M.C.d.A. (conceptualization, formal analysis, funding acquisition, investigation, project administration, supervision, writing—review and editing). All authors have read and agreed to the published version of the manuscript.

Funding: This research was funded by Brazilian Agricultural Research Corporation (EMBRAPA), grants number 12.14.04.002.00.00 and 20.22.03.013.00.00; the São Paulo Research Foundation (FAPESP), grants number 2021/05092-7 and 2017/22401-8; the Brazilian National Council for Scientific and Technological Development (CNPq), grant number 406925/2022-4, 308777/2021-2 (INCT Circularity in Polymer Materials), 303329/2022-0, and 308777/2021-2 (Research Productivity Fellowships); Coordination for the Improvement of Higher Education Personnel (CAPES), scholarships number 88882.180323/2018-01 and 88887.619942/2021-00.

Data Availability Statement: The data used to support the findings of this study can be made available by the authors upon request.

Acknowledgments: The authors gratefully acknowledge the financial support by the Brazilian Agricultural Research Corporation (EMBRAPA, 12.14.04.002.00.00 and 20.22.03.013.00.00), São Paulo Research Foundation (FAPESP, 2021/05092-7 and 2017/22401-8), and the Brazilian National Council for Scientific and Technological Development (CNPq, INCT Circularity in Polymer Materials, 406925/2022-4). Authors Ribeiro and Barros thank the Coordination for the Improvement of Higher Education Personnel (CAPES) for their scholarships (88882.180323/2018-01, and 88887.619942/2021-00, respectively). Authors Rosa and Azeredo thank the National Council for Scientific and Technological Development (CNPq) for their Research Productivity Fellowships (303329/2022-0 and 302950/2025-7, respectively).

Conflicts of Interest: The authors declare no conflicts of interest.

References

1. United Nations General Assembly Resolution A/RES/79/1 (The Pact for the Future). Adopted 22 September 2024. Available online: https://docs.un.org/en/A/RES/79/1 (accessed on 14 September 2025).
2. Rosenboom, J.G.; Langer, R.; Traverso, G. Bioplastics for a Circular Economy. *Nat. Rev. Mater.* **2022**, *7*, 117–137. [CrossRef]
3. Brussels: European Commission Energy, Climate Change, Environment. Available online: https://commission.europa.eu/energy-climate-change-environment_en (accessed on 14 September 2025).
4. Wang, B.; Yan, S.; Gao, W.; Kang, X.; Yu, B.; Liu, P.; Guo, L.; Cui, B.; Abd El-Aty, A.M. Antibacterial Activity, Optical, and Functional Properties of Corn Starch-Based Films Impregnated with Bamboo Leaf Volatile Oil. *Food Chem.* **2021**, *357*, 129743. [CrossRef]
5. Combrzyński, M.; Wójtowicz, A.; Oniszczuk, A.; Karcz, D.; Szponar, J.; Matwijczuk, A.P. Selected Physical and Spectroscopic Properties of TPS Moldings Enriched with Durum Wheat Bran. *Materials* **2022**, *15*, 5061. [CrossRef] [PubMed]
6. Alonso-González, M.; Felix, M.; Romero, A. Influence of the Plasticizer on Rice Bran-Based Eco-Friendly Bioplastics Obtained by Injection Moulding. *Ind. Crops Prod.* **2022**, *180*, 114767. [CrossRef]
7. Waterschoot, J.; Gomand, S.V.; Delcour, J.A. Impact of Swelling Power and Granule Size on Pasting of Blends of Potato, Waxy Rice and Maize Starches. *Food Hydrocoll.* **2016**, *52*, 69–77. [CrossRef]
8. Abegunde, O.K.; Mu, T.H.; Chen, J.W.; Deng, F.M. Physicochemical Characterization of Sweet Potato Starches Popularly Used in Chinese Starch Industry. *Food Hydrocoll.* **2013**, *33*, 169–177. [CrossRef]
9. Kasemwong, K.; Ruktanonchai, U.R.; Srinuanchai, W.; Itthisoponkul, T.; Sriroth, K. Effect of High-Pressure Microfluidization on the Structure of Cassava Starch Granule. *Starch/Staerke* **2011**, *63*, 160–170. [CrossRef]
10. Gamage, A.; Liyanapathiranage, A.; Manamperi, A.; Gunathilake, C.; Mani, S.; Merah, O.; Madhujith, T. Applications of Starch Biopolymers for a Sustainable Modern Agriculture. *Sustainability* **2022**, *14*, 6085. [CrossRef]

11. Choudhary, P.; Devi, T.B.; Tushir, S.; Kasana, R.C.; Popatrao, D.S.; Narsaiah, K. Mango Seed Kernel: A Bountiful Source of Nutritional and Bioactive Compounds. *Food Bioproc. Technol.* **2023**, *16*, 289–312. [CrossRef]
12. Todhanakasem, T.; Jaiprayat, C.; Sroysuwan, T.; Suksermsakul, S.; Suwapanich, R.; Maleenont, K.K.; Koombhongse, P.; Young, B.M. Active Thermoplastic Starch Film with Watermelon Rind Extract for Future Biodegradable Food Packaging. *Polymers* **2022**, *14*, 3232. [CrossRef]
13. Melo, P.E.F.; Silva, A.P.M.; Marques, F.P.; Ribeiro, P.R.V.; Souza Filho, M.d.s.M.; Brito, E.S.; Lima, J.R.; Azeredo, H.M.C. Antioxidant Films from Mango Kernel Components. *Food Hydrocoll.* **2019**, *95*, 487–495. [CrossRef]
14. Silva, A.P.M.; Oliveira, A.V.; Pontes, S.M.A.; Pereira, A.L.S.; Souza Filho, M.d.s.M.; Rosa, M.F.; Azeredo, H.M.C. Mango Kernel Starch Films as Affected by Starch Nanocrystals and Cellulose Nanocrystals. *Carbohydr. Polym.* **2019**, *211*, 209–216. [CrossRef]
15. Gomez-Caturla, J.; Ivorra-Martinez, J.; Quiles-Carrillo, L.; Balart, R.; Garcia-Garcia, D.; Dominici, F.; Puglia, D.; Torre, L. Improvement of the Barrier and Mechanical Properties of Environmentally Friendly Mango Kernel Flour/Glycerol Films by Varying the Particle Size of Mango Kernel Flour. *Ind. Crops Prod.* **2022**, *188*, 115668. [CrossRef]
16. Gomez-Caturla, J.; Ivorra-Martinez, J.; Lascano, D.; Balart, R.; García-García, D.; Dominici, F.; Puglia, D.; Torre, L. Development and Evaluation of Novel Nanofibers Based on Mango Kernel Starch Obtained by Electrospinning. *Polym. Test.* **2022**, *106*, 107462. [CrossRef]
17. Barros, M.d.O.; Mattos, A.L.A.; Almeida, J.S.d.; Rosa, M.d.F.; Brito, E.S.d. Effect of Ball-Milling on Starch Crystalline Structure, Gelatinization Temperature, and Rheological Properties: Towards Enhanced Utilization in Thermosensitive Systems. *Foods* **2023**, *12*, 2924. [CrossRef]
18. *ASTM D638-14*; Standard Test Method for Tensile Properties of Plastics. ASTM International: West Conshohocken, PA, USA, 2014. [CrossRef]
19. *ASTM D570-98*; Standard Test Method for Water Absorption of Plastics. ASTM International: West Conshohocken, PA, USA, 2018. [CrossRef]
20. Lyu, Y.; Gu, X.; Mao, Y. Green Composite of Instant Coffee and Poly(Vinyl Alcohol): An Excellent Transparent UV-Shielding Material with Superior Thermal-Oxidative Stability. *Ind. Eng. Chem. Res.* **2020**, *59*, 8640–8648. [CrossRef]
21. Mahadi, F.M.; Mustafa, S.E.; Saad, O.M.; Hamdi, O.A. Evaluation of Nutritional Value and Bioactive Ingredients of Oil. *Acta Sci. Med. Sci.* **2020**, *4*, 190–196. [CrossRef]
22. Yang, N.; Gao, W.; Zou, F.; Tao, H.; Guo, L.; Cui, B.; Lu, L.; Fang, Y.; Liu, P.; Wu, Z. The Relationship between Molecular Structure and Film-Forming Properties of Thermoplastic Starches from Different Botanical Sources. *Int. J. Biol. Macromol.* **2023**, *230*, 123114. [CrossRef]
23. Gomez-Caturla, J.; Ivorra-Martinez, J.; Fenollar, O.; Balart, R.; Garcia-Garcia, D.; Dominici, F.; Puglia, D.; Torre, L. Development of Starch-Rich Thermoplastic Polymers Based on Mango Kernel Flour and Different Plasticizers. *Int. J. Biol. Macromol.* **2024**, *264*, 130773. [CrossRef] [PubMed]
24. Mansaray, K.G.; Ghaly, A.E. Determination of Kinetic Parameters of Rice Husks in Oxygen Using Thermogravimetric Analysis. *Biomass Bioenergy* **1999**, *17*, 19–31. [CrossRef]
25. Dai, L.; Zhang, J.; Cheng, F. Effects of Starches from Different Botanical Sources and Modification Methods on Physicochemical Properties of Starch-Based Edible Films. *Int. J. Biol. Macromol.* **2019**, *132*, 897–905. [CrossRef]
26. Ferraz, C.A.; Fontes, R.L.S.; Fontes-Sant'Ana, G.C.; Calado, V.; López, E.O.; Rocha-Leão, M.H.M. Extraction, Modification, and Chemical, Thermal and Morphological Characterization of Starch From the Agro-Industrial Residue of Mango (*Mangifera indica* L) Var. Ubá. *Starch/Staerke* **2019**, *71*, 1800023. [CrossRef]
27. Socrates, G. *Infrared and Raman Characteristic Group Frequencies: Tables and Charts*, 3rd ed.; Wiley & Sons: New York, NY, USA, 2004.
28. Liu, W.; Wang, Z.; Liu, J.; Dai, B.; Hu, S.; Hong, R.; Xie, H.; Li, Z.; Chen, Y.; Zeng, G. Preparation, Reinforcement and Properties of Thermoplastic Starch Film by Film Blowing. *Food Hydrocoll.* **2020**, *108*, 106006. [CrossRef]
29. Mansour, G.; Zoumaki, M.; Marinopoulou, A.; Tzetzis, D.; Prevezanos, M.; Raphaelides, S.N. Characterization and Properties of Non-Granular Thermoplastic Starch—Clay Biocomposite Films. *Carbohydr. Polym.* **2020**, *245*, 116629. [CrossRef]
30. Zullo, R.; Iannace, S. The Effects of Different Starch Sources and Plasticizers on Film Blowing of Thermoplastic Starch: Correlation among Process, Elongational Properties and Macromolecular Structure. *Carbohydr. Polym.* **2009**, *77*, 376–383. [CrossRef]
31. Ma, S.; Zhu, P.; Wang, M. Effects of Konjac Glucomannan on Pasting and Rheological Properties of Corn Starch. *Food Hydrocoll.* **2019**, *89*, 234–240. [CrossRef]
32. Ma, H.; Liu, M.; Liang, Y.; Zheng, X.; Sun, L.; Dang, W.; Li, J.; Li, L.; Liu, C. Research Progress on Properties of Pre-Gelatinized Starch and Its Application in Wheat Flour Products. *Grain Oil Sci. Technol.* **2022**, *5*, 87–97. [CrossRef]
33. Manoel, A.F.; Claro, P.I.C.; Mattoso, L.H.C.; Marconcini, J.M.; Mantovani, G.L. Thermoplastic Waxy Starch Films Processed by Extrusion and Pressing: Effect of Glycerol and Water Concentration. *Mater. Res.* **2017**, *20*, 353–357. [CrossRef]

34. Guzman-Puyol, S.; Hierrezuelo, J.; Benítez, J.J.; Tedeschi, G.; Porras-Vázquez, J.M.; Heredia, A.; Athanassiou, A.; Romero, D.; Heredia-Guerrero, J.A. Transparent, UV-Blocking, and High Barrier Cellulose-Based Bioplastics with Naringin as Active Food Packaging Materials. *Int. J. Biol. Macromol.* **2022**, *209*, 1985–1994. [CrossRef] [PubMed]
35. Sá, N.M.S.M.; Mattos, A.L.A.; Silva, L.M.A.; Brito, E.S.; Rosa, M.F.; Azeredo, H.M.C. From Cashew Byproducts to Biodegradable Active Materials: Bacterial Cellulose-Lignin-Cellulose Nanocrystal Nanocomposite Films. *Int. J. Biol. Macromol.* **2020**, *161*, 1337–1345. [CrossRef]